Influence of electron-phonon interaction on the lattice thermal conductivity of $Co_{1-x}Ni_xSb_3$

J. Yang,[1] D. T. Morelli,[2] G. P. Meisner,[1] W. Chen,[3] J. S. Dyck,[3] and C. Uher[3]
[1]*Materials and Processes Laboratory, GM R&D and Planning, Warren, Michigan 48090*
[2]*Delphi Automotive Systems Research Labs, Shelby Township, Michigan 48315*
[3]*Department of Physics, University of Michigan, Ann Arbor, Michigan 48109*
(Received 27 June 2001; published 21 February 2002)

We have investigated the effect of electron-phonon scattering in a series of n-type nickel-doped $CoSb_3$ skutterudite materials. Samples were polycrystalline of the form $Co_{1-x}Ni_xSb_3$ with $x=0$, 0.001, 0.003, 0.005, 0.0075, and 0.01. The lattice thermal conductivity decreases dramatically with increasing Ni doping for $x \leqslant 0.003$. For higher Ni concentration the reduction of the lattice thermal conductivity saturates. Our theoretical analysis indicates that this reduction of the lattice thermal conductivity cannot be explained solely by point-defect scattering of the phonons. Rather, we can fit the lattice thermal conductivity of Ni-doped $CoSb_3$ by introducing an electron-phonon scattering mechanism, and this demonstrates that the electron-phonon interaction can play an important role in the reduction of the heat conduction in n-type skutterudites.

DOI: 10.1103/PhysRevB.65.094115 PACS number(s): 63.20.Kr, 66.70.+f

INTRODUCTION

The interest in skutterudites as potential thermoelectric materials in recent years has drawn a lot of attention to their fundamental transport parameters: electrical resistivity, thermopower, and thermal conductivity. The physical properties of skutterudites and their optimization for thermoelectric applications have been summarized in two recent reviews.[1,2] A good thermoelectric material has to have a large figure of merit defined as $ZT=S^2T/\rho\kappa$, where S is the thermopower, ρ is the electrical resistivity, κ is the total thermal conductivity, and T is the temperature. The binary (unfilled) skutterudites have moderate power factors (S^2/ρ), but the thermal conductivity is too high. Slack proposed the phonon-glass-electron-crystal (PGEC) approach of reducing the thermal conductivity by filling voids in the skutterudite crystal structure with rare-earth atoms without deteriorating their electrical properties,[3] and this was validated in a number of filled skutterudites[4–6] that led to ZT approaching 1.4 around 900 K.[7,8] An understanding of the phonon scattering mechanism in skutterudites has attracted a lot of attention because of both its technological implications and its intriguing physics. Feldman *et al.*[9] suggested that the anharmonic scattering by harmonic rare-earth filler motions is an important mechanism for the suppression of heat conduction in filled skutterudites. Meisner *et al.*[10] found that mass fluctuations between the fully filled and unfilled subphases of the optimum filled skutterudites can explain the lattice thermal conductivity minimum as a function of the filling fraction. We learned that the dominant factor of heat conduction suppression in Fe-doped $CoSb_3$ is point-defect scattering.[11,12] Room-temperature lattice thermal conductivity of Ni-doped $CoSb_3$ was reported by Anno *et al.*,[13] where the dominant phonon scattering mechanism was attributed to electron-phonon interactions. In this paper, we present our low-temperature (2–300 K) lattice thermal conductivity data on a series of Ni-doped samples, and it is in this temperature region that the effect of the electron-phonon interaction can be clearly differentiated from other phonon scattering mechanisms.

EXPERIMENTAL TECHNIQUES

Polycrystalline samples of the form $Co_{1-x}Ni_xSb_3$ were fabricated by a combination of arc melting and induction melting of high-purity constituents. The Ni concentrations are 0, 0.001, 0.003, 0.005, 0.0075, and 0.01. The ingots were annealed at 700 °C for 20 h. Samples were analyzed by x-ray powder diffraction and electron probe microanalysis. Transport property measurements were performed in a cryostat equipped with a radiation shield from 2 to 300 K using a steady-state technique,[14] and the typical sample size for transport measurements was $3\times3\times10$ mm^3.

RESULTS AND DISCUSSION

Our x-ray powder diffraction and electron probe microanalysis (EPMA) results indicate that all samples are single phase and have compositions very close to the desired stoichiometry. Table I lists the nominal compositions and the compositions determined by EPMA.

The lattice thermal conductivity κ_L was derived by subtracting the electronic thermal conductivity κ_e from the measured total thermal conductivity κ. The electronic thermal conductivity was estimated from the Wiedemann-Franz law using a value for the Lorenz number of 2.45×10^{-8} V^2/K^2 and, for all the samples, κ_e was less than 2% of κ. Figure 1 displays the temperature dependence of κ_L from 2 to 300 K for the $Co_{1-x}Ni_xSb_3$ samples, and it is clear that Ni doping

TABLE I. Nominal compositions and EPMA-determined compositions for $Co_{1-x}Ni_xSb_3$.

Nominal compositions	EPMA compositions
$CoSb_3$	$CoSb_{3.0225}$
$Co_{0.999}Ni_{0.001}Sb_3$	$Co_{0.999}Ni_{0.0009}Sb_{3.0102}$
$Co_{0.997}Ni_{0.003}Sb_3$	$Co_{0.997}Ni_{0.0031}Sb_{3.0559}$
$Co_{0.995}Ni_{0.005}Sb_3$	$Co_{0.995}Ni_{0.0049}Sb_{2.9862}$
$Co_{0.9925}Ni_{0.0075}Sb_3$	$Co_{0.9925}Ni_{0.0076}Sb_{2.9987}$
$Co_{0.99}Ni_{0.01}Sb_3$	$Co_{0.99}Ni_{0.01}Sb_{3.0309}$

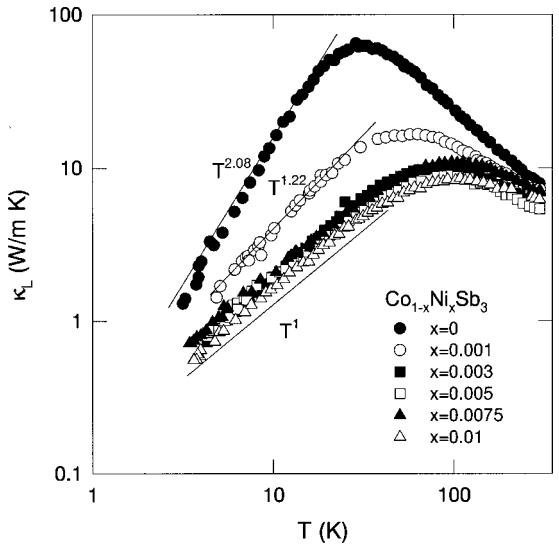

FIG. 1. Temperature dependence of the lattice thermal conductivity of $Co_{1-x}Ni_xSb_3$ from 2 to 300 K. The lines indicate that κ_L is proportional to $T^{2.08}$, $T^{1.22}$, and T^1 between 2 and 30 K for $x=0$, 0.001, and 0.003, respectively.

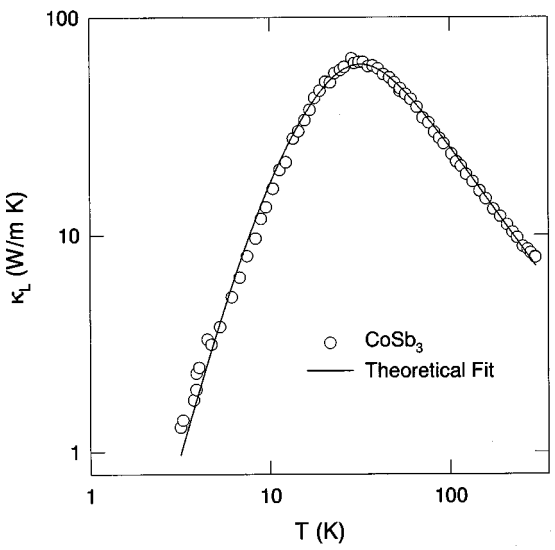

FIG. 2. Lattice thermal conductivity for $CoSb_3$ vs temperature. The open circles are experimental data, and the line is the calculation based on Eqs. (1) and (2).

strongly suppresses κ_L. For very small Ni concentrations ($x \leqslant 0.003$), κ_L decreases rapidly with increasing x, and this effect is especially manifested at low temperature ($T < 100$ K). As the Ni concentration increases, the suppression of κ_L seems to saturate. In Fig. 1 the lines are drawn to illustrate the T^a dependence of κ_L at low temperature ($T < 30$ K), where $a=2.08$, 1.22, and 1 for $x=0$, $x=0.001$, and $x \geqslant 0.003$, respectively. For pure $CoSb_3$, our theoretical analysis (which will be discussed later in this paper) suggests that electron-phonon scattering is negligible, and this agrees with our previous results for $CoSb_3$ in our Fe-doped $CoSb_3$ study.[11] Grain boundary scattering, at sufficiently low temperatures, will dominate and κ_L will have a T^3 dependence. The observed $\kappa_L \propto T^{2.08}$ indicates the presence of point-defect scattering in addition to grain-boundary scattering for temperatures down to 2 K. Consequently, one would have to extend the measurements into the sub-kelvin range to observe $\kappa_L \propto T^3$.

We performed theoretical fits of the lattice thermal conductivity for all $Co_{1-x}Ni_xSb_3$ samples using the following expression:[15]

$$\kappa_L = \frac{k_B}{2\pi^2 v}\left(\frac{k_B T}{\hbar}\right)^3 \int_0^{\theta_D/T} \frac{x^4 e^x}{\tau_C^{-1}(e^x-1)^2}\,dx, \qquad (1)$$

where $x=\hbar\omega/k_B T$ is dimensionless, ω is the phonon frequency, k_B is the Boltzmann constant, $\hbar$ is the reduced Planck constant, θ_D is the Debye temperature, v is the velocity of sound, and τ_C is the phonon scattering relaxation time. The phonon scattering relaxation rate τ_C^{-1} can be written as

$$\tau_C^{-1} = \frac{v}{L} + A\omega^4 + B\omega^2 T \exp\left(-\frac{\theta_D}{3T}\right) + C\omega^2, \qquad (2)$$

where L is the grain size and the coefficients A, B, and C are the fitting parameters. The terms in Eq. (2) represent grain-boundary scattering, point-defect scattering, phonon-phonon umklapp scattering, and electron-phonon scattering, respectively. The partial relaxation rate for the electron-phonon interaction was derived by Pippard[16] when working on the ultrasonic attenuation of metals. According to Eqs. (1) and (2), κ_L will be proportional to T^1 in the temperature range where the electron-phonon scattering dominates, and this is what we observe in Fig. 1 at low temperature ($T < 30$ K) for samples with high Ni concentrations ($x \geqslant 0.003$).

As we have shown in Fig. 1, κ_L for $x \geqslant 0.003$ is almost unchanged. No additional physics can be elucidated upon displaying the fits for $x > 0.003$. Figures 2–4 show the experimental lattice thermal conductivity with the theoretical fit for $CoSb_3$, $Co_{0.999}Ni_{0.001}Sb_3$, and $Co_{0.997}Ni_{0.003}Sb_3$, respec-

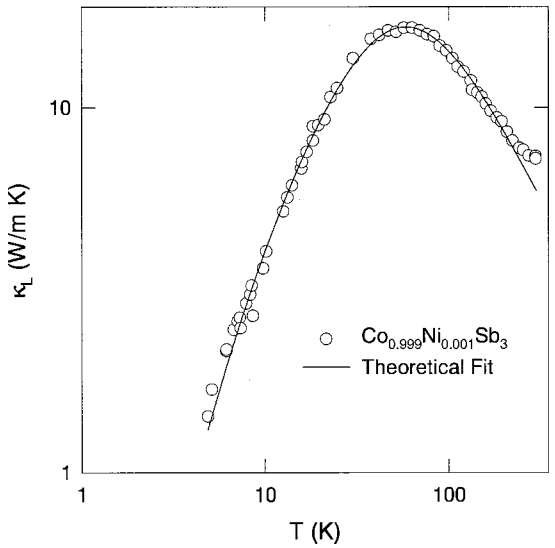

FIG. 3. The lattice thermal conductivity for $Co_{0.999}Ni_{0.001}Sb_3$ vs temperature. The open circles are experimental data and the line is the calculation based on Eqs. (1) and (2).

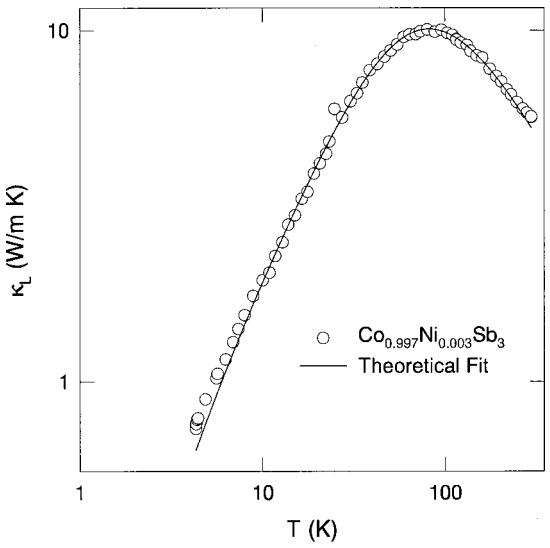

FIG. 4. The lattice thermal conductivity for $Co_{0.997}Ni_{0.003}Sb_3$ vs temperature. The open circles are experimental data, and the line is the calculation based on Eqs. (1) and (2).

tively, and the resulting fitting parameters are listed in Table II. We fixed the prefactor *B* for the phonon-phonon umklapp scattering for all the samples to be the same as that we used for fitting Fe-doped $CoSb_3$.[11,12] The grain sizes emerging from the fits are very close to those determined from backscatter electron imaging and optical micrography, which are also listed in Table II. The theoretical model fits the experimental data very well in the temperature range from 2 to 300 K. A small deviation from the solid line fit is observed for $Co_{0.999}Ni_{0.001}Sb_3$ near room temperature, Fig. 3, and this may be due to radiation losses.[12,14] There is no obvious trend for the prefactor *A* for point-defect scattering as a function of Ni concentration. The prefactor *C* for the electron-phonon interaction, however, increases significantly upon Ni doping. Here *C* can be written as[16]

$$C=\frac{4nm^*v_e\lambda_e}{15dv^2}, \tag{3}$$

where n is the electron concentration, m^* is the effective electron mass, v_e is the electron velocity, λ_e is the mean free path of the electrons, and d is the mass density. Equation (3) is valid when $q\lambda_e \ll 1$, where $q=2\pi/\lambda_p$ is the phonon wave vector and λ_p is the phonon wavelength. So Eq. (3) is valid only if the wavelength of the phonons is longer than the electron mean free path. The conventional theory of the influence of electron-phonon interaction on lattice conduction in semimetals and semiconductors uses matrix element method.[17] This formulation of the electron-phonon interaction is based on the adiabatic principle and perturbation theory. The criterion for the validity of the theory is $q\lambda_e \gg 1$. For the $Co_{1-x}Ni_xSb_3$ samples we studied, at low temperature the electron mean free path is much shorter than the phonon wavelength, as we estimated below. Hence we expect the break down of the perturbation theory or the adiabatic approximation. Even though the theory by Pippard[16] was originally developed to explain ultrasonic attenuation of metals, and even though it is classical in nature, it successfully reproduced the results of the electron-phonon interaction for semimetals and semiconductors by quantum methods in the case of $q\lambda_e \gg 1$.[17] We expect that Eq. (3) drawn from the same Pippard's general formula for the other limiting case, i.e., $q\lambda_e \ll 1$, should also be valid for semiconductors. More importantly, in our $Co_{1-x}Ni_xSb_3$ series, we believe the experimental result of $\kappa_L \propto T^1$ at low temperature for $x \geqslant 0.003$ is a demonstration of the validity of Eq. (3). Since the electron-phonon interaction is manifested at low temperature, we will use the low-temperature data to estimate the prefactor *C* of the electron-phonon interaction. From our analysis of the electrical transport and magnetic data,[18] we learn that the electrical conduction at low temperature (less than 30 K) is dominated by hopping of electrons among the impurity states. The electron mean free path is equal to the average distance between Ni atoms and can therefore be estimated as $\lambda_e=(xn_{\mathrm{Co}})^{-1/3}$, where $n_{\mathrm{Co}}=1.1\times10^{22}$ cm^{-3} is the number of Co atoms/cm^3. The estimated electron mean free path for Ni-doped samples is on the order of 10^{-9} m, which is much shorter than the estimated phonon wavelength $\sim10^{-8}$ m by the dominant phonon method[19] in the low-temperature region ($T<30$ K). We therefore expect the Pippard model to be valid. In case of electron-phonon interaction between the electrons in the conduction band and the lattice phonons, v_e can normally be replaced by the Fermi velocity v_F. For $Co_{1-x}Ni_xSb_3$ at low temperatures, however, an electron-phonon interaction occurs between the impurity electrons and the lattice phonons. We thus replace v_e by $v_e=\lambda_e/\tau_e$, and use $\mu_e=e\tau_e/m^*$, where τ_e and μ_e are electron scattering relaxation time and mobility, respectively. Equation (3) can therefore be replaced by

$$C=\frac{4ne\lambda_e^2}{15dv^2\mu_e}. \tag{4}$$

The variables on the right-hand side of Eq. (4) can then be estimated by experimentally determined values. The impurity band mobility is usually several orders of magnitude

TABLE II. Fit parameters *L*, *A*, *B*, and *C* for the lattice thermal conductivity of $CoSb_3$, $Co_{0.999}Ni_{0.001}Sb_3$, and $Co_{0.997}Ni_{0.003}Sb_3$ using Eqs. (1) and (2), and the average grain size L_{expt} determined by backscatter electron imaging and optical micrography.

Sample	L (μm)	A (10^{-43} s^3)	B (10^{-18} s K^{-1})	C (10^{-18} s)	L_{expt} (μm)
$CoSb_3$	5.772	2.591	5.375	2.796	5.5±1.7
$Co_{0.999}Ni_{0.001}Sb_3$	7.731	5.659	5.375	157.6	6.2±2.2
$Co_{0.997}Ni_{0.003}Sb_3$	10.69	3.385	5.375	458.7	5.8±2.0

TABLE III. Room-temperature carrier concentrations and effective masses (estimated from room-temperature thermopower and carrier concentration of each sample) for $Co_{1-x}Ni_xSb_3$ (Ref. 18).

Nominal composition	Carrier concentration (cm^{-3})	$m^*(m_e)$
$CoSb_3$	3.70×10^{17}	0.175
$Co_{0.999}Ni_{0.001}Sb_3$	-3.33×10^{18}	3.60
$Co_{0.997}Ni_{0.003}Sb_3$	-9.75×10^{18}	3.35
$Co_{0.995}Ni_{0.005}Sb_3$	-1.18×10^{19}	3.07
$Co_{0.9925}Ni_{0.0075}Sb_3$	-2.52×10^{19}	3.92
$Co_{0.99}Ni_{0.01}Sb_3$	-3.26×10^{19}	3.76

lower than that of the conduction band. The magnetic field that we used for our Hall measurement is not strong enough to detect the contribution from the electrons in the impurity band. We believe that the experimentally determined mobility in Ref. 18 is characteristic of the conduction band. The electron mobility of the impurity band can be estimated as $\mu_e=\mu_c/b$, where the conduction band mobility μ_c and the values of b can be found in Ref. 18. We take $d=7.58\ \mathrm{g/cm^3}$ and $v=2700\ \mathrm{m/s}$.[11,12] We use the room-temperature carrier concentration listed in Table III for n, since the majority of the carriers are frozen into the impurity level at low temperature.[18] The calculated C values for $x=0.001$ and 0.003 are 7.41×10^{-16} s and 3.49×10^{-16} s, respectively. Even though the calculated C values do not have a definite composition dependence, they do predict the right order of magnitude. A very large effective mass and a very low mobility are characteristics of impurity conduction. We expect the electron effective mass in the impurity band to be several orders of magnitude larger than that of the conduction band, though we are unable to make a good estimate. From this analysis we conclude that the reduction in lattice thermal conductivity (especially at low temperature) is the result of an electron-phonon interaction between the very heavy impurity electrons and the lattice phonons.

We have also calculated the values of C by using experimentally determined parameters for the electrons in the conduction band. They are several orders of magnitude smaller than that calculated for the impurity electrons. This implies that the electron-phonon interaction between the conduction electrons and the lattice phonons is not a significant factor for determining the lattice thermal conductivity near room temperature, where the majority of the electrons are in the conduction band. The strong electron-phonon interaction at low temperatures would likely cause changes in the phonon spectrum, which inevitably leads to different umklapp scattering coefficients. We speculate that this is the reason for the observed 30% variation in the lattice thermal conductivity at room temperature among all the samples.

Table III lists the room-temperature carrier concentrations and effective masses (estimated from room-temperature thermopower and carrier concentration of each sample) for all $Co_{1-x}Ni_xSb_3$ samples. According to Ref. 18, the pure $CoSb_3$ sample is p type and its effective mass is $0.175m_e$, where m_e is the free electron mass. A very small amount of Ni doping (even with $x=0.001$) converts the electrical conductivity to n-type. The effective mass of the n band is about 30 times larger than that of the p band. At low temperature, electrical transport is dominated by the impurity band formed by Ni impurities. In our attempt to fit the lattice thermal conductivity of the pure $CoSb_3$ sample shown in Fig. 2, we could have fit the overall temperature dependence without the electron-phonon interaction term, and the resulting fitting parameters L,A, and B are not significantly different from those in Table II. This indicates that the electron-phonon interaction in pure $CoSb_3$ is not a significant factor for determining the lattice thermal conductivity. The effective mass for the valence band in skutterudites is very small, $\sim0.175m_e$. The electron-phonon interaction in p-type $Co_{1-x}Fe_xSb_3$ is therefore not significant. The much heavier impurity band not only significantly enhances the thermopower,[18] but also gives rise to the much stronger electron-phonon interaction. The prefactor C for the electron-phonon interaction emerging from our theoretical fit (listed in Table II) increases by two orders of magnitude from the pure to the doped samples with increasing Ni concentration up to $x=0.003$. For samples with higher Ni concentrations ($x>0.003$), the lattice thermal conductivity is not reduced further, as can be seen in Fig. 1. We speculate that this might be because the increasing electron-phonon interaction eventually exhausts the number of phonons available in the frequency region where the electron-phonon interaction dominates.[20] Recently, Sales *et al.*[21] reported the room-temperature lattice thermal conductivity of 5.71 W/m K for a $Co_{0.95}Ni_{0.05}Sb_3$ sample with $5\times10^{20}\ \mathrm{cm^{-3}}$ electron concentration. This value is very close to that of our $Co_{0.99}Ni_{0.01}Sb_3$ sample, further corroborating the saturation of the lattice thermal conductivity reduction above $x=0.003$.

SUMMARY

We have measured the lattice thermal conductivity of a series of samples of the form $Co_{1-x}Ni_xSb_3$ with $x=0$, 0.001, 0.003, 0.005, 0.0075, and 0.01 from 2 to 300 K. We observed that the lattice thermal conductivity κ_L is strongly suppressed upon Ni doping. The $\kappa_L\propto T^1$ relation is observed from 2 to 30 K for samples with $x=0.003$ and higher Ni doping, indicating that a strong electron-phonon interaction is present. Our theoretical calculation fits the overall temperature dependence of the lattice thermal conductivity very well. The much heavier electron effective mass of the impurity band gives rise to a very strong electron-phonon interaction in the Ni-doped samples. Therefore, the reduction of the heat conduction due to the electron-phonon interaction in n-type skutterudites cannot be neglected.

ACKNOWLEDGMENTS

We want to thank Professor P. G. Klemens and Professor G. A. Slack for valuable discussions. J.Y. and G.P.M. want to thank Dr. J. F. Herbst and Dr. K. C. Taylor for encouragement and support during this work, and Richard Waldo for the EPMA measurements. This work is also supported in part by DARPA under Contract No. N00014-98-3-0011.

[1] G. S. Nolas, D. T. Morelli, and T. M. Tritt, Annu. Rev. Mater. Sci. **29**, 89 (1999).
[2] C. Uher, in *Semiconductors and Semimetals*, edited by T. M. Tritt (Academic, San Diego, CA, 2000), Vol. 69, p. 139.
[3] G. A. Slack and V. G. Tsoukala, J. Appl. Phys. **76**, 1665 (1994).
[4] D. T. Morelli and G. P. Meisner, J. Appl. Phys. **77**, 3777 (1995).
[5] G. S. Nolas, G. A. Slack, D. T. Morelli, T. M. Tritt, and A. C. Ehrlich, J. Appl. Phys. **79**, 4002 (1996).
[6] B. C. Sales, D. Mandrus, and R. K. Williams, Science **272**, 1325 (1996).
[7] J.-P. Fleurial, A. Borshchevsky, T. Caillat, D. T. Morelli, and G. P. Meisner, in *Proceedings of the 15th International Conference Thermoelectrics* (IEEE, Piscataway, NJ, 1996), p. 91.
[8] J.-P. Fleurial, A. Borshchevsky, T. Caillat, D. T. Morelli, and G. P. Meisner, U.S. Patent No. 6,069,312 (2000).
[9] J. L. Feldman, D. J. Singh, I. I. Mazin, and B. C. Sales, Phys. Rev. B **61**, 9209 (2000).
[10] G. P. Meisner, D. T. Morelli, S. Hu, J. Yang, and C. Uher, Phys. Rev. Lett. **80**, 3551 (1998).
[11] J. Yang, D. T. Morelli, G. P. Meisner, and C. Uher, in *Thermal Conductivity 25/Thermal Expansion 13*, edited by C. Uher, and D. T. Morelli (Technomic, Lancaster, PA, 2000), p. 130.
[12] J. Yang, G. P. Meisner, D. T. Morelli, and C. Uher, Phys. Rev. B **63**, 014410 (2001).
[13] H. Anno, K. Matsubara, Y. Notohara, T. Sakakibara, and H. Tashiro, J. Appl. Phys. **86**, 3780 (1999).
[14] J. Yang, Ph.D. thesis, University of Michigan, Ann Arbor, MI, 2000.
[15] J. Callaway, Phys. Rev. **113**, 1046 (1959).
[16] A. B. Pippard, Philos. Mag. **46**, 1104 (1955).
[17] J. M. Ziman, *Electrons and Phonons* (Clarendon, Oxford, UK, 1960).
[18] J. S. Dyck, W. Chen, J. Yang, G. P. Meisner, and C. Uher, Phys. Rev. B (to be published 15 March 2002).
[19] R. Berman, *Thermal Conduction in Solids* (Oxford University Press, Oxford, UK, 1976).
[20] G. A. Slack (private communication).
[21] B. C. Sales, B. C. Chakoumakos, and D. Mandrus, Phys. Rev. B **61**, 2475 (2000).